Journal of Molecular Liquids 391 (2023) 123188

Contents lists available at ScienceDirect

Journal of Molecular Liquids

journal homepage: www.elsevier.com/locate/molliq

Surface tension, wettability and tribological properties of a low viscosity oil using $CaCO_3$ and CeF_3 nanoparticles as additives

José M. Liñeira del Río [a,b,*], Alonso Alba [a], María J.G. Guimarey [a], Jose I. Prado [c], Alfredo Amigo [d], Josefa Fernández [a]

[a] Laboratory of Thermophysical and Tribological Properties, Nafomat Group, Department of Applied Physics, Faculty of Physics, and Institute of Materials (iMATUS), Universidade de Santiago de Compostela, 15782 Santiago de Compostela, Spain
[b] Unidade de Tribologia, Vibraçoes e Manutençao Industrial, INEGI, Universidade do Porto, Porto, Portugal
[c] CINBIO, Universidade de Vigo, Grupo GAME, Departamento de Física Aplicada, 36310 Vigo, Spain
[d] Laboratory of Thermophysical and Surface Properties of Liquids, Department of Applied Physics, Faculty of Physics, University of Santiago de Compostela, 15782 Santiago de Compostela, Spain

ARTICLE INFO

Keywords:
Lubricants
EV systems
Nanoparticles
Transmissions

ABSTRACT

The rise of the electric vehicles as a more sustainable transport alternative makes it necessary to study new transmission fluids that adapt to their needs and improve their efficiency. The thermophysical properties (contact angle, surface tension and rheology) and tribological properties (friction and wear) of potential PAO8 transmission nanofluids using $CaCO_3$ and CeF_3 nanoparticles as additives are evaluated at mass concentrations of 0.05, 0.10, 0.15 and 0.20 wt%. Low contact angle and surface tension values are obtained, indicating good wettability. When the nanoparticles are used as PAO8 additives, small reductions in surface tension are achieved, but no differences in contact angle are observed. All nanolubricants and base oil exhibit Newtonian behavior. Concerning the tribological behavior, reductions in the friction coefficient are achieved for both types of nanoparticles, with the largest reductions comparing to PAO8 base oil being 13 % and 10 % for nanolubricants containing 0.05 wt% $CaCO_3$ and 0.10 wt% CeF_3 nanoparticles (NPs), respectively. In terms of antiwear performance, maximum reductions are obtained for the $CaCO_3$ nanolubricant of 28 % (0.15 wt%), 41 % (0.10 wt%) and 59 % (0.15 wt%) and for the CeF_3 nanolubricant of 19 % (0.20 wt%), 53 % (0.10 wt%) and 58 % (0.20 wt%) for the parameters of diameter, depth, and area of the worn track, respectively. Through Raman microscopy, the tribological mechanisms of tribofilm formation, repairing, and rolling can be proposed. A discontinuous tribofilm formed by the $CaCO_3$ and CeF_3 nanoparticles reduces the contact area between the two surfaces protecting them.

1. Introduction

Nowadays, electric vehicles (EVs) have become increasingly important for reducing fuel use as well as pollution of air. To enhance more this positive outcome, it is crucial to improve their behavior. One possible way is to enhance the tribological performance of the mechanical elements and of the lubricants of the transmission power system. In many EVs, the electric motor and transmission are in the same cover, in which case the electric transmission fluids (ETF) must a) have a low viscosity; b) have capability to do not allow copper corrosion and also be compatible with polymers, and c) exhibit suitable electrical properties [1–4]. Low viscosity lubricants are used owing to the high operating speeds and torque of mechanical components in EVs. Viscous drag as well as viscous heating reduce and heat transfer improves when the oil viscosity is reduced [5,6]. Nevertheless, if the viscosity of the lubricant decreases, the change from full film to boundary lubrication could occur, probably leading to critical surface contact and cause significant wear. Therefore, advanced lubricants with good anti-wear and antifriction properties are required. In this vein, an efficacious method to decrease friction and wear is using nanomaterials as lubricant

* Corresponding author at: Laboratory of Thermophysical and Tribological Properties, Nafomat Group, Department of Applied Physics, Faculty of Physics, and Institute of Materials (iMATUS), Universidade de Santiago de Compostela, 15782 Santiago de Compostela, Spain.
E-mail address: josemanuel.lineira@usc.es (J.M. Liñeira del Río).

https://doi.org/10.1016/j.molliq.2023.123188
Received 12 July 2023; Received in revised form 17 September 2023; Accepted 25 September 2023
Available online 26 September 2023

Table 1
Main physical properties of PAO8 [38].

Nature	Density at 313.15 K / g cm^{-3}	Dynamic Viscosity at 313.15 K / mPa s	Viscosity index
Synthetic	0.8163	39.47	138

additives [7–12]; achieving decreases in losses of energy, wear as well as pollutant emissions. There are numerous reasons for using nanoparticles (NPs) as lubricant additives but most important is that because of their small size, NPs can enter in the contact area, resulting in positive lubrication effects [13]. In addition, NPs as lubricant additives can act through different lubrication mechanisms: rolling effect and tribo-film formation owing to direct effect of the nanoparticle on the surface and mending and polishing effects due to surface enhancement [14]. Moreover, the suitable nanoparticles used as additives should be less chemically reactive than traditional additives, as their films are formed mechanically, so they will be more durable and less reactive with other additives [15]. Another advantage of using NPs as lubricant additives is their low volatility, which avoids losses at high temperature conditions [15].

Another important quality of transmission fluids is their ability to spread on a metal surface, and their wettability. Wettability is usually characterized through property measurements such as contact angle or surface tension, being relevant to study its dependence on temperature. This type of studies can be found for different fluids such as ionic liquids [16] or lubricants [17]. Currently, there are hardly any studies on the effect of the nanoadditives on the wettability properties (contact angle and surface tension) of nanolubricants [18], although there are studies of NPs in water [19,20]. It is therefore of particular interest to known how these properties are affected by the addition of different concentrations of NPs.

Polyalphaolefins (PAOs) are widely used in various applications owing to their excellent competence as base oils and their thermal and oxidative stability, which leads to enhanced performance in comparison with mineral oils [5]. Thus, Thampi et al. [21] and Mariño et al. [22] reviewed the effect of NPs and chemically modified NPs, respectively, on the tribological properties of various lubricating oils, including PAOs, observing important tribological improvements with different NPs. Specifically, Mariño et al. [22] found that the best tribological performance in PAOs was obtained with Pd [23], TiO_2 [24] and SiO_2 [25] NPs with friction and wear reductions around 40 % and 90 %, respectively. Furthermore, Mustafa et al. [5] reviewed some few articles on low-viscosity nanolubricants, including those based on low-viscosity PAOs, finding remarkable results in friction and wear. Mustafa et al. [5] and Thampi et al. [21] observed that the best tribological performance was obtained by Kalin et al. [26] using MoS_2 NPs as additives of PAO6, reducing the friction coefficient by more than two times, while the wear was reduced by five-nine times. In this work, polyalphaolefin 8 (PAO8) was selected as the base oil because its performance for electric transmissions and for its low viscosity [27]. Regarding the nanoadditives, $CaCO_3$ and CeF_3 NPs were used as additives of the PAO8 base oil. $CaCO_3$ NPs are environmentally friendly and verify the European Ecolabel criteria for use as lubricant additives [57]. $CaCO_3$ NPs are generally used in the automotive industry, in construction, in plastic seals, adhesives, paints, and inks. There are numerous studies on the use of calcium carbonate NPs as grease additives [29–31]. However, the literature on $CaCO_3$ NPs as lubricating oil additives is scarce [32–34]. Zhang et al.

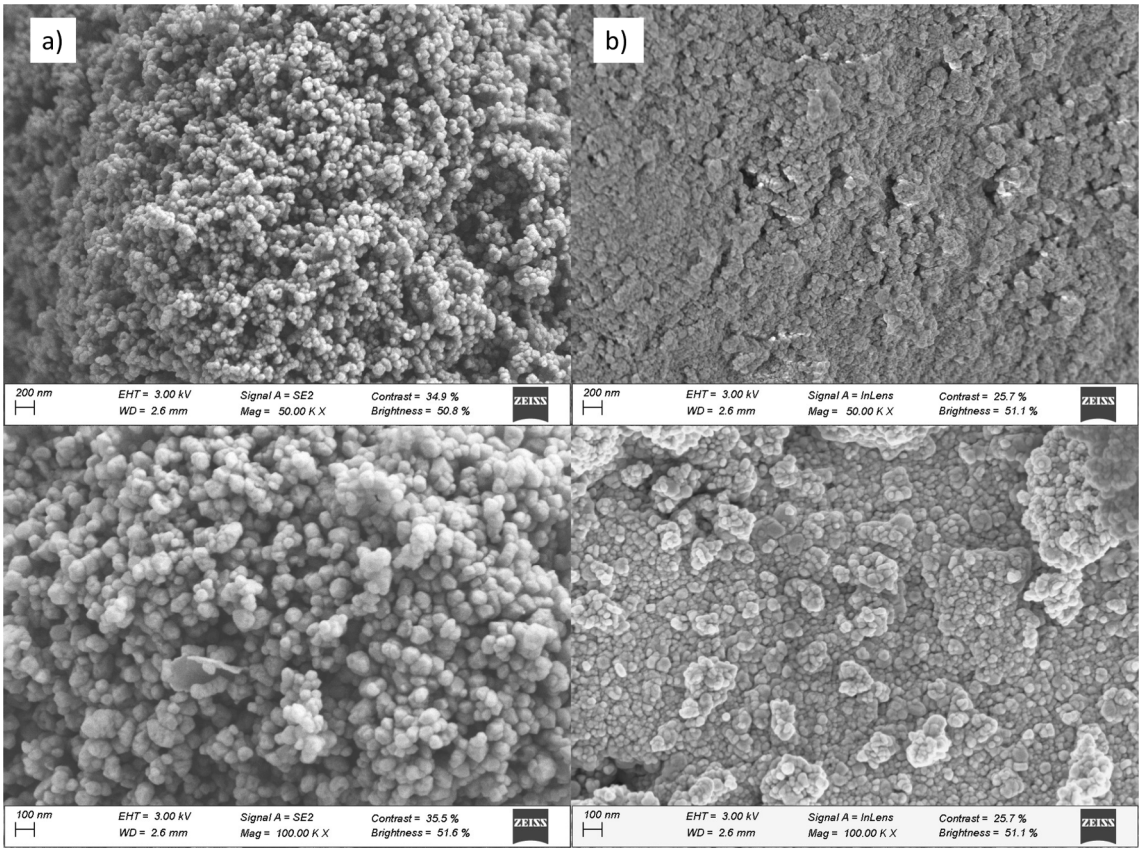

Fig. 1. SEM images of a) $CaCO_3$ and b) CeF_3 nanopowders.

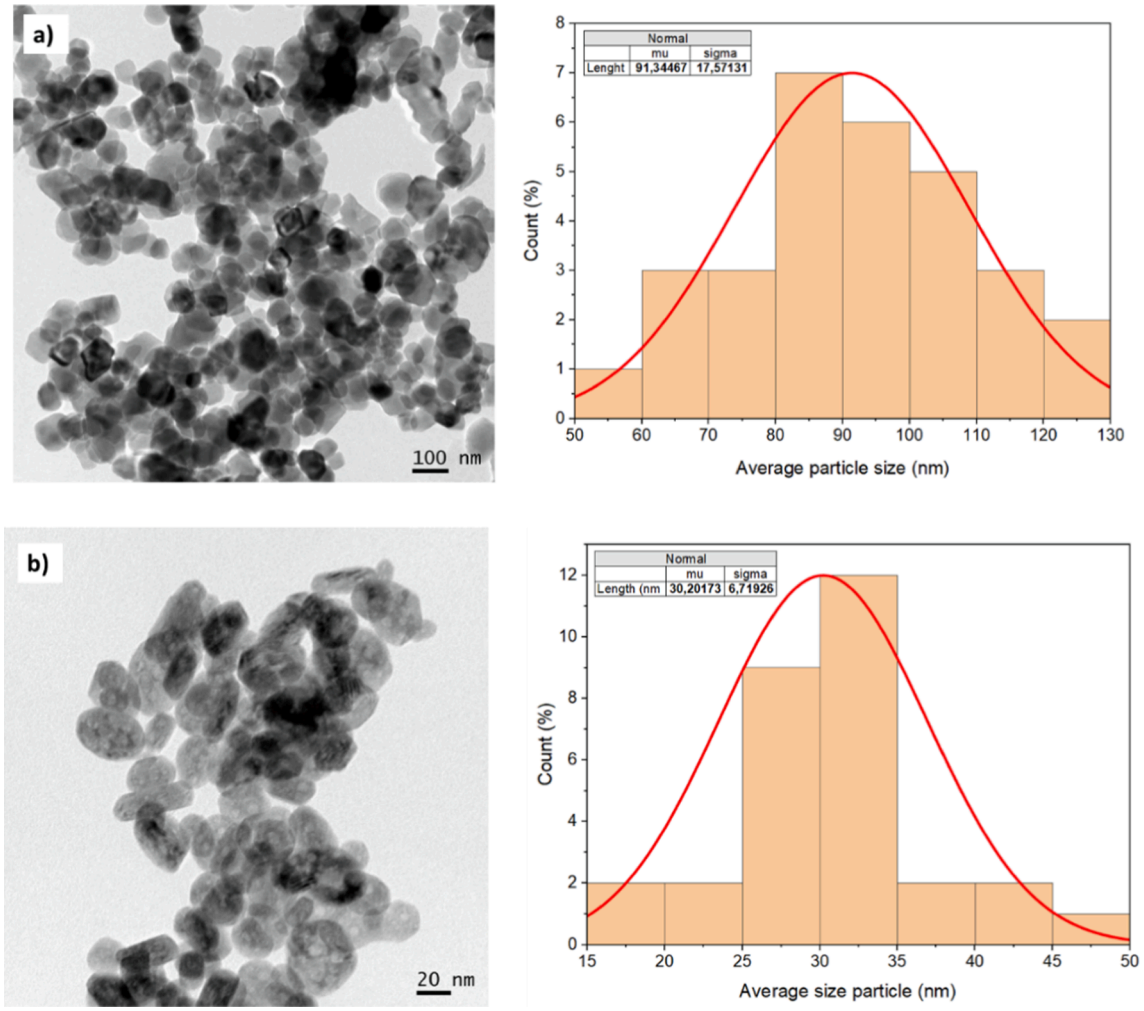

Fig. 2. TEM images and size nanoparticles distribution of a) $CaCO_3$ and b) CeF_3 nanopowders.

[35] studied the tribological behavior of $CaCO_3$ NPs as an environmentally friendly additive to PAO10 base oil, showing that $CaCO_3$ NPs can considerably enhance the load carrying capability and the anti-wear and anti-friction-reducing properties of a PAO10 base oil (88 % reduction in wear volume). Kulkarni et al. [36] have investigated green nanolubricants dispersing different mass concentrations of $CaCO_3$ NPs in jojoba oil, finding that the addition of $CaCO_3$ NPs in the oil reveals remarkable anti-wear and extreme-pressure properties, with maximum decreases in coefficient of friction and wear scar diameter of balls around 35 % and 40 %, respectively.

It is worth mentioning that currently there are hardly any literature articles that use CeF_3 NPs as lubricant additives [37]. Sunqing et al. [37] synthesized this type of NPs using a microemulsion of water, cyclohexane and polybutene diamide, achieving NPs with an average size of 25 nm, which were added to a 500SN oil-based lubricant. Tribological results showed a significant reduction in the coefficient of friction (about 25 %) and a slight reduction in wear. Considering all the above, it is important to develop new potential low viscosity nanolubricants particularly adapted to EVs and CeF_3 and $CaCO_3$ NPs may be excellent candidates to be used as additives for further study. Thus, in this work surface tension, wettability and tribological properties of potential electric transmission nanofluids based on PAO8 oil containing $CaCO_3$ or CeF_3 NPs as additives are evaluated at mass concentrations of 0.05, 0.10, 0.15 and 0.20 wt%.

2. Material and experimental methods

2.1. Materials

The polyalphaolefin 8 base oil, PAO8, was provided by REPSOL. As shown in Table 1, this base oil has a dynamic viscosity and density at 313.15 K of 39.47 mPa s and 0.8163 g cm^{-3}, respectively, and a viscosity index of 138 [38]. The PAO8 base oil was previously characterized using Fourier-transform infrared spectroscopy (FTIR) as well as Raman spectroscopy [38].

Concerning the nanoadditives, $CaCO_3$ and CeF_3 NPs were delivered by US Research Nanomaterials, Inc. (Houston, TX USA). The $CaCO_3$ NPs have a purity of 98 %, an average diameter of 50 nm, and a specific surface area of 40–80 m^2/g. Furthermore, CeF_3 NPs have a size of 20 nm and a purity of 99.99 %. Scanning Electron Microscopy (SEM, Zeiss FESEM Ultra Plus) and Transmission Electron Microscopy (JEOL JEM-F200CF-HR) were used to know the aspect and dimension of both

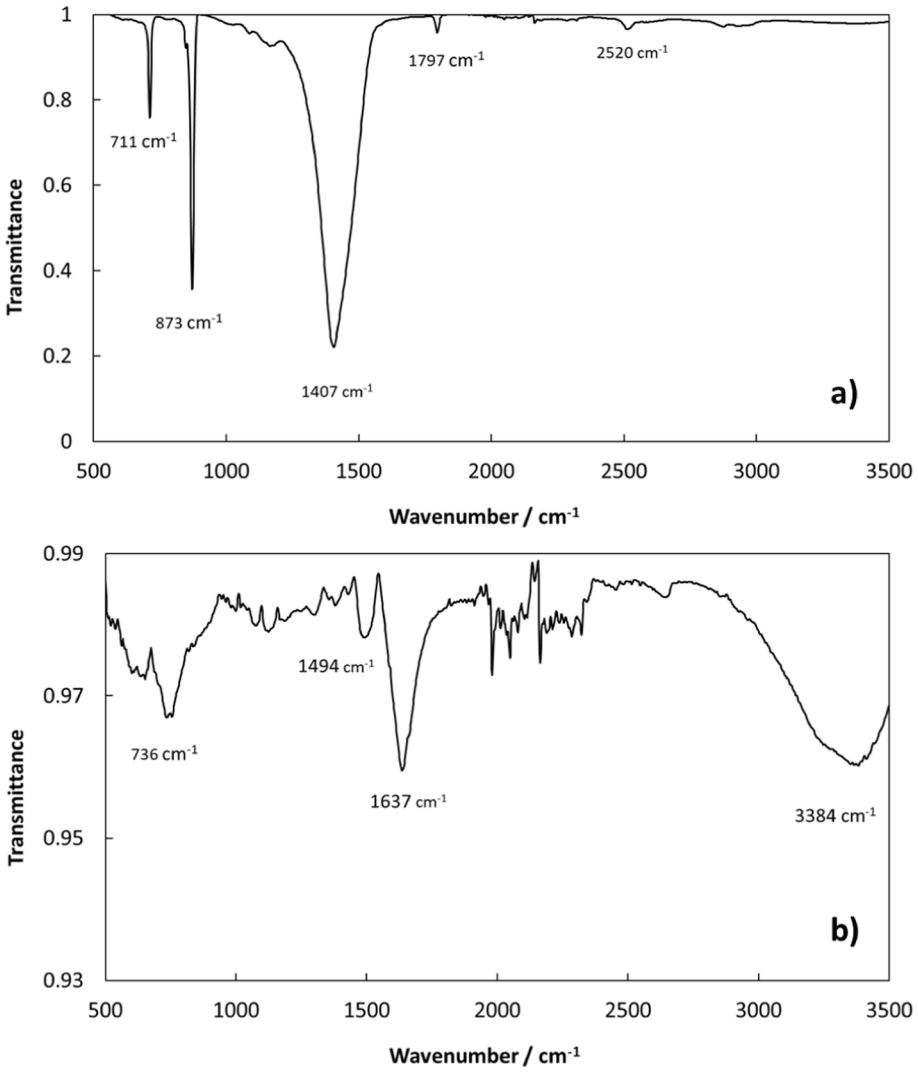

Fig. 3. FT-IR spectrum of $CaCO_3$ (a) and CeF_3 (b) NPs.

types of NPs. As Figs. 1 and 2 illustrate, both NPs ($CaCO_3$ and CeF_3) have a spherical shape, especially in the case of $CaCO_3$ NPs. Regarding the nanoparticle sizes, it can be observed that $CaCO_3$ NPs have a larger size than CeF_3 NPs. Specifically, Fig. 2 shows the size distribution of both NPs (obtained with ImageJ), observing that the average sizes for the $CaCO_3$ and CeF_3 NPs are around 91 nm and 30 nm, respectively.

The $CaCO_3$ and CeF_3 NPs were also characterized by FTIR to determine the bonds associated with each NP. The FTIR spectra of $CaCO_3$ and CeF_3 NPs are shown in Fig. 3. The first one shows three prominent peaks around 710 cm^{-1}, 875 cm^{-1} and 1405 cm^{-1} corresponding respectively to a deformation in the plane, to a deformation outside in-plane and doubly degenerate in-plane strain typical of $CaCO_3$ [39,40]. On the other hand, the spectrum of CeF_3 NPs shows peaks detected at 736 cm^{-1}, 1494 cm^{-1}, 1637 cm^{-1} and 3384 cm^{-1} [41].

Raman spectroscopy of both nanopowders was used to identify the characteristic absorption bands, Fig. 4. The $CaCO_3$ spectrum, Fig. 4a, shows a very strong Stokes band at 1087 cm^{-1} and weaker ones at 160 cm^{-1}, 286 cm^{-1}, 716 cm^{-1} and 2950 cm^{-1}, which were also found in a spectrum of the corresponding bulk material, $CaCO_3$ [42]. On the other hand, Fig. 4b shows the Raman spectrum of the CeF_3 NPs. In this spectrum there are two pronounced bands at 309 cm^{-1} and 566 cm^{-1} and other less intense bands at 993 cm^{-1} and 1094 cm^{-1}, which match with the spectrum of the corresponding bulk material, CeF_3 [41].

$CaCO_3$ and CeF_3 NPs were also characterized by X-Ray diffraction (XRD) to determine the crystalline form of both NPs. For this aim, a Bruker D8 Advance with Cu-Kα radiation ($\lambda = 1.5418$ nm) was used at room temperature. The XRD patterns were carried out between $2\theta = 3$-80°. The Debye-Scherrer's formula was applied to calculate the crystallite size of the nanoparticles based on the following equation [43]:

$$Dp = K\lambda/(Bcos\theta) \quad (1)$$

where Dp, K, λ, B, and θ are the average crystallite size, the Scherrer constant, the entire width at the half summit of the diffraction peak, and the Bragg angle of the peak. Fig. 5 shows the XRD pattern of the $CaCO_3$ and CeF_3 NPs. In the $CaCO_3$ XRD pattern, Fig. 5a, peaks are found at 2θ = 23.1°, 29.41°, 35.98°, 39.42°, 43.16°, 47.52° and 48.52°, corresponding to (012), (104), (110), (113), (202), (018) and (016) crystal planes [44]. The experimental XRD pattern agrees with the ICSD

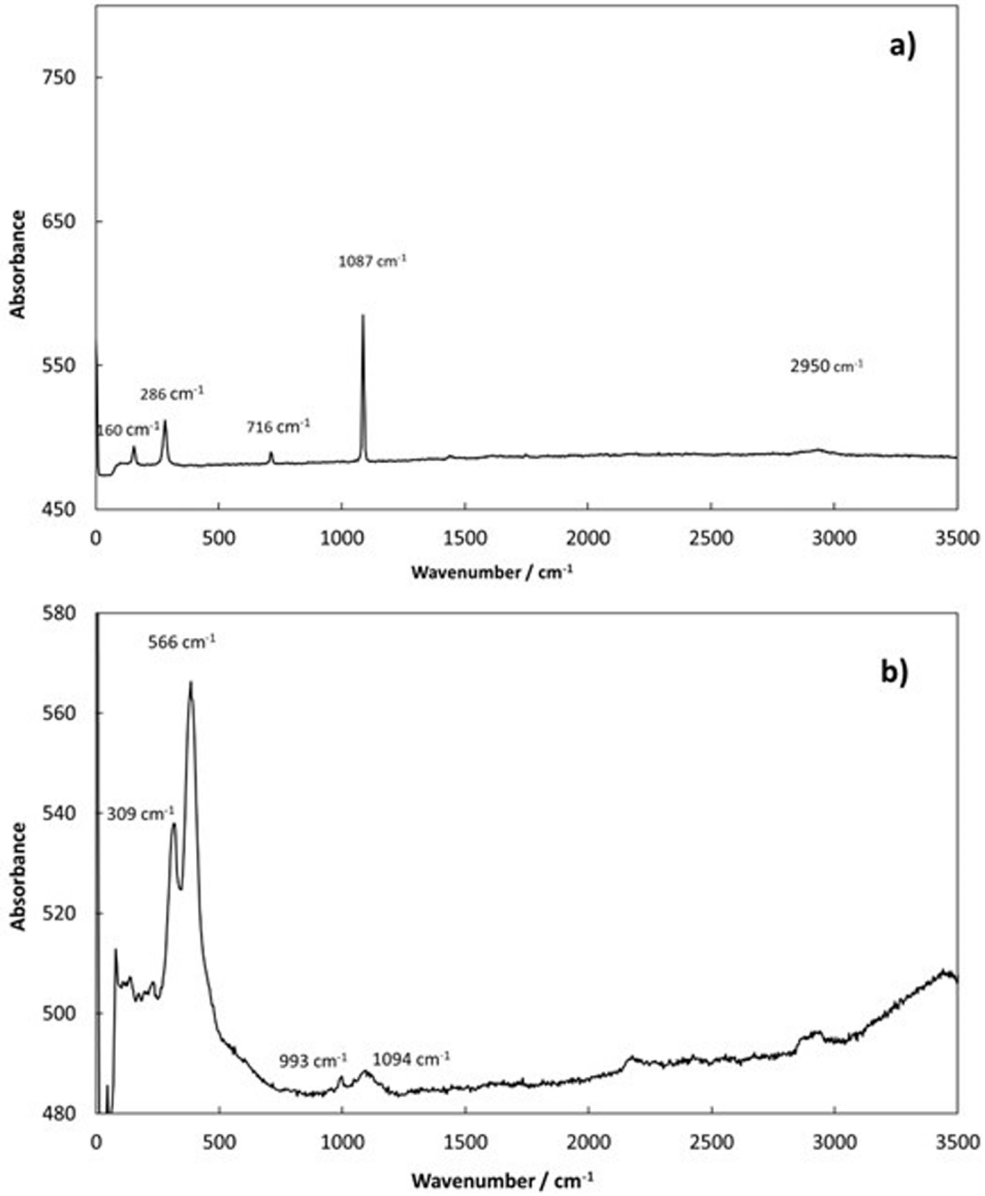

Fig. 4. Raman spectrum of $CaCO_3$ (a) and CeF_3 (b) NPs.

Card No: 98–004-0107 (Calcite) [44]. The crystallite size of $CaCO_3$ NPs determined from the above peaks using the Eq. (1) is 96.68 nm.

Regarding the XRD pattern of CeF_3 NPs (Fig. 5.b), peaks are found at $2\theta = 24.38°$, 24.93°, 27.81°, 43.93°, 45.10°, 50.92°, 52.80° and 64.80°. The experimental XRD pattern is in accordance with the ICSD Card No: 98–006-4720 (Fluocerite) [45]. The crystallite size of CeF_3 NPs calculated from these peaks using the Eq. (1) is 25.01 nm.

2.2. Preparation of nanolubricants

Nanolubricants were made according to the conventional two-step procedure [22]. Firstly, dry nanopowders ($CaCO_3$ or CeF_3 NPs) were mixed with PAO8 base oil, determining the mass concentrations through a Sartorius MC 210P balance. For this purpose, the base oil was weighed and then the amount of nanopowder required to achieve the desired mass concentrations was also weighed. Secondly, the homogenization of nanodispersions was carried out first with a mechanical stirrer (Fisherbrand Vortex) for 2 min and finally with an ultrasonic bath (Fisherbrand FB11203 from Fisher Scientific, USA) for 4 h. It should be noted that the preparation process the nanolubricants (formulation and homogenization) is relatively short (around 6 h). To find out the optimum mass concentration with the highest tribological behavior, eight nanodispersions of PAO8 were prepared with the following nanoadditives: + 0.05 wt% $CaCO_3$, + 0.10 wt% $CaCO_3$, + 0.15 wt% $CaCO_3$, + 0.20 wt% $CaCO_3$, + 0.05 wt% CeF_3, + 0.10 wt% CeF_3, + 0.15 wt% CeF_3 and + 0.20 wt% CeF_3.

2.3. Stability of nanolubricants

To control the stability of the NPs within the oil, a simple setup is used, where the samples of nanolubricants are placed with good lighting on a background of the opposite color to that of the sample for better

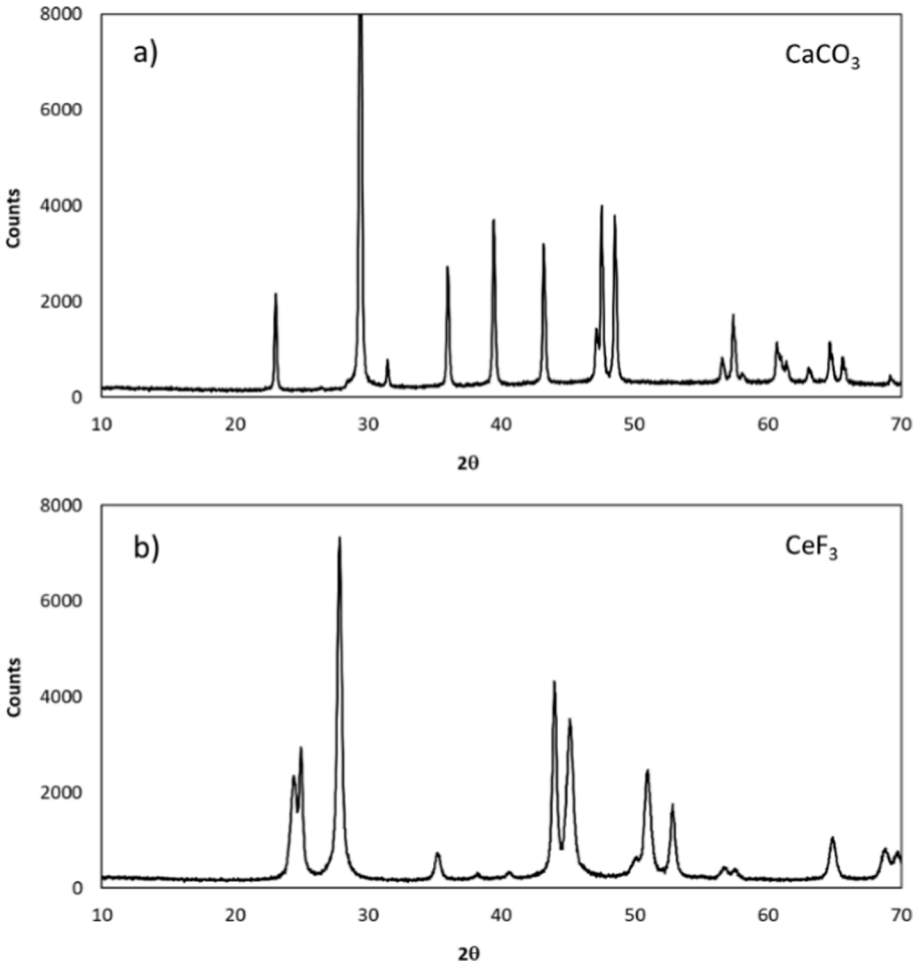

Fig. 5. XRD pattern of $CaCO_3$ (a) and CeF_3 (b) NPs.

visualization. The process consists in that once the nanodispersion is prepared and homogenized, it is not manipulated, and a series of photographs are taken periodically at room temperature, to detect when the NPs are deposited. In this case, a black background is used, and photographs were taken approximately every 24 h. Furthermore, to analyze stability more quantitative, the evolution of the refractive index over time was measured by means of a refractometer (Mettler Toledo RA-510 M).

2.4. Surface tension, contact angle and rheology

To carry out the surface tension measurements, a Lauda TVT 2 Drop Volume Tensiometer was used, which allows measuring the surface tension through the volume of the falling drop following Tate's law [46]. The fluid sample is introduced into a syringe of 2.5 mL volume, being expelled from it through a needle of 1.370 mm inner radius. The temperature of the lubricant sample in the syringe is controlled with a thermal bath to maintain it at 298.15 or 313.15 K. The uncertainty in the measured temperature was $u(T)/\mathrm{K} = 0.03$. For each surface tension experiment, 30 to 40 drops are used to obtain a mean volume value with good reproducibility. The uncertainty in surface tension measurements depends on the nanolubricant ranging between 0.05 and 0.2 mN m^{-1}.

A Phoenix MT-A analyzer was utilized to achieve the contact angle of all the lubricants on AISI 420 stainless steel plates. For the calibration of the equipment camera, a glass plate supplied by the manufacturer is used, which contains reference graduation marks for different contact angles. The lubricant is introduced into a syringe which, with the help of the equipment's motor, makes a drop of lubricant fall on the steel plate previously cleaned with acetone. It should be noted that this plate is placed on a surface that is thermostated with a bath to keep the desired temperature during the analysis time. The uncertainty in the measured temperature was $u(T)/\mathrm{K} = 0.5$. The obtained result is the evolution of the contact angle over time, specifically its value every second for 1 min (a series of 60 values). Several series of measurements are carried out for each oil, ensuring the correct repeatability of the contact angles, taking the average of all the values. The estimated uncertainty in the contact angle measurements is 2 %.

The rheological behavior of the PAO8 base oil and its nanolubricants containing $CaCO_3$ and CeF_3 NPs was investigated with an Anton Paar MCR 101 rheometer (Graz, Austria) at 293.15, 333.15, and 363.15 K. The rheometer is equipped with a cone-plate geometry with a cone diameter of 50 mm and a cone angle of 1°. The cone went down to an imposed gap of 0.102 mm from the plate and covered the whole sample for all tests. Furthermore, the temperature is controlled by means a Peltier P-PTD 200 (Anton Paar, Graz, Austria), set at the lower plate, with a diameter of 56 mm. Further details of this apparatus can be found in a previous article [47]. Flow curves of tested lubricants were recorded in the shear rate range from 10 to 1000 s^{-1}. The expanded uncertainty of

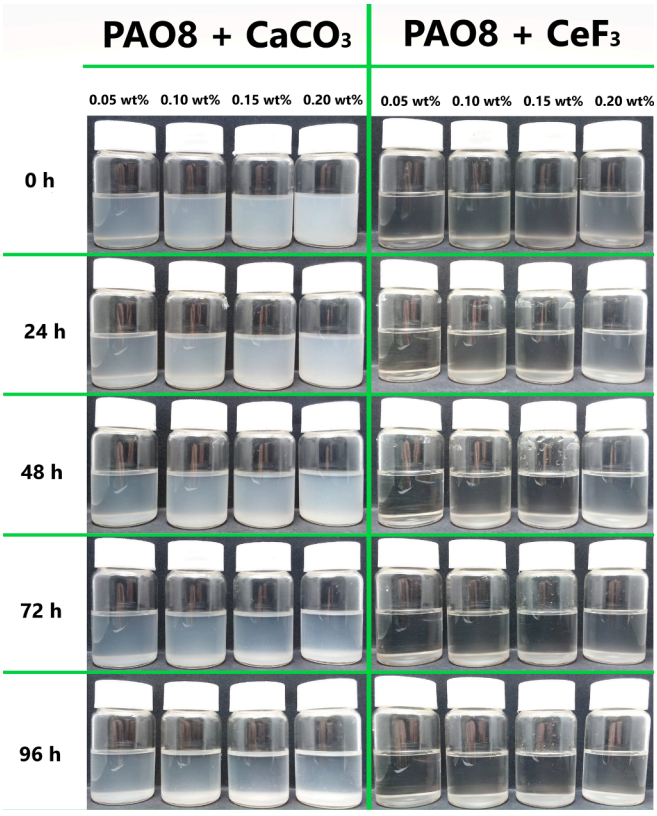

Fig. 6. Stability control performed on the different nanolubricants of $CaCO_3$ and CeF_3.

viscosity measurement is estimated to be better than 5 % (k = 2) [47]. It should be noted that an amount of 0.59 mL of sample was considered for the analysis and was placed on the Peltier plate.

2.5. Tests of friction and wear examination

Ball-on-three pins friction tests with PAO8 base oil and with the eight $CaCO_3$ and CeF_3 nanolubricants were performed through a Peltier heated T-PTD200 tribology unit in an Anton Paar MCR 302 rheometer (Graz, Austria). The ball is placed in a vertical tube that is powered by the motor of the rheometer, while the pins, situated at the base of the holder, are touching the ball at an angle of 45° with the tube. During the friction tests, the ball that supports a vertical axial force applied by the rheometer, turns on the pins. This force (20 N) gives rise to three identical normal forces (9.43 N) that action perpendicularly on the surfaces of the three pins. In each pin, the maximum Hertzian pressure corresponds to 1.1 GPa [48]. Pins with 6 mm radius and 6 mm height, and balls with 12.7 mm diameter were utilized, being both components of 100Cr6 hardened steel (hardness Rockwell C between 66 and 62). The friction tests were performed at rotational speed of 213 rpm (ball surface velocity being 0.1 m s^{-1}), for 3400 s for a 393.15 K temperature. Approximately 1 mL of lubricant was utilized in each test in order to cover the contact surface. More information on this tribological apparatus can be found in earlier articles [49,50]. The temperature was selected since for great operation of EV motors, a high-power density is necessary and so the heat generation in the coil improves. Nonetheless, to avoid demagnetization, the temperature must be below 150 °C. More information on these issues was reported by Rodriguez et al. [4].

When the friction tests for each lubricant were completed (3 repeats for each one), the wear was estimated in pins, to investigate which nanolubricant offers the best anti-wear performance. Pins were cleaned with a hexane stream and dried with hot air before the wear analysis. A 3D profilometer (Sensofar, S-Neox) was used to measure various worn track parameters: wear scar diameter (WSD), wear track depth (WTD), worn area and roughness. It should be noted that the worn area was determined using the section profile by subtracting from the worn area the sum of areas of the profiles for the material displaced on both sides of the worn track. All the parameters were determined in all the pins tested with all the lubricant samples to obtain appropriate mean values. Moreover, a confocal Raman microscope (WITec alpha300R+) was used to obtain information of the chemical organization in the worn scar and

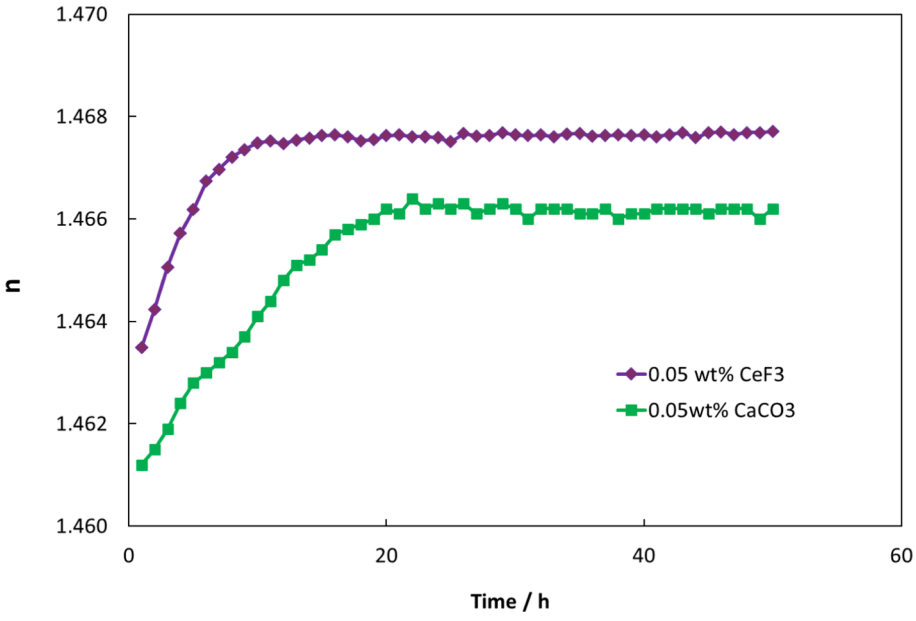

Fig. 7. Refractive index evolution for 0.05 wt% $CaCO_3$ and CeF_3 nanolubricants.

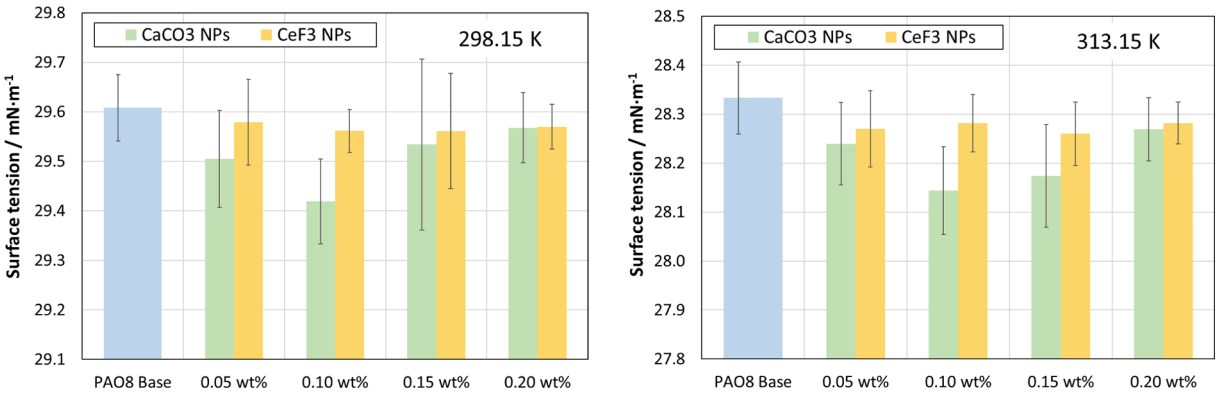

Fig. 8. Surface tension obtained for the base oil and its nanolubricants containing $CaCO_3$ or CeF_3 NPs at different mass fractions, wt%, at 298.15 and 313.15 K.

Table 2
Surface tension, γ, and its uncertainties, σ, of the formulated nanolubricants and the PAO8 base oil.

	298.15 K		313.15 K	
	γ/mN m^{-1}	σ/mN m^{-1}	γ/mN m^{-1}	σ/mN m^{-1}
PAO8 Base	29.61	0.07	28.33	0.07
+0.05 wt% $CaCO_3$	29.51	0.10	28.24	0.08
+0.10 wt% $CaCO_3$	29.42	0.09	28.14	0.09
+0.15 wt% $CaCO_3$	29.53	0.17	28.17	0.10
+0.20 wt% $CaCO_3$	29.57	0.07	28.27	0.06
+0.05 wt% CeF_3	29.58	0.09	28.27	0.08
+0.10 wt% CeF_3	29.56	0.04	28.28	0.06
+0.15 wt% CeF_3	29.56	0.12	28.26	0.07
+0.20 wt% CeF_3	29.57	0.05	28.28	0.04

to gain insight into the tribological mechanisms that may happen.

3. Results and discussion

3.1. Stability results

The photos corresponding to the visual stability control of the nanodispersions are shown in Fig. 6. Both NPs are stable in the PAO8 base oil for at least 48 h, which is a sufficient stability time to carry out the tribological and thermophysical tests. It should be noted that Fig. 6 also shows that the stability decreases for both NPs when the mass concentration increases.

The other method used to analyze the stability of the formulated nanolubricants against sedimentation is refractometry. Fig. 7 shows the evolution of the refractive index for the $CaCO_3$ and CeF_3 nanolubricants, both with a NP concentration of 0.05 wt%. It can be clearly observed that for the 0.05 wt% CeF_3 nanolubricant after the first ten hours NPs are full sedimented, whereas in the case of the 0.05 wt% $CaCO_3$ nanolubricant the sedimentation is quite gradual. More precisely, for the first nanolubricant the refractive index increased 0.28 % after 10 h and for the $CaCO_3$ nanolubricant it increased 0.19 %. It should be noted that for low viscosity oils is more difficult to find good stabilities than for viscous oils, since the nanoparticles have less resistance to falling in oil.

3.2. Surface tension, contact angle and rheology results

Fig. 8 and Table 2 show the values of surface tension, γ, obtained for the nanolubricants with the four mass concentrations $CaCO_3$ or CeF_3 NPs and the PAO8 base oil at temperatures of 298.15 K and 313.15 K. It can be observed that the surface tensions of the nanodispersions are slightly lower than those of PAO8 at both temperatures. In particular, for the samples containing CeF_3 NPs the variation is almost negligible. For the case of 0.15 wt% decreases of 0.16 % for $T = 298.15$ K and 0.26 % for $T = 313.15$ K were found. On the other hand, for the nanolubricants containing $CaCO_3$ NPs, the difference is greater, showing a minimum at 0.10 wt% with reductions of 0.64 % for $T = 298.15$ K and 0.67 % for $T = 313.15$ K. Currently, there are hardly any studies related to wettability properties (contact angle and surface tension) when nanoparticles are added to lubricants [18], although there are several studies of nanoparticles in water [19,20]. Therefore, it is critical to study how these properties are affected by the addition of different concentrations of nanoparticles.

Regarding the contact angle, Fig. 9 shows the measurements of the nanolubricants with $CaCO_3$ and CeF_3 NPs and of the base PAO8 without additives. No clear trend is observed in any of the cases that could indicate a significant change in the angle values of contact by the addition of NPs. It is worth mentioning that the differences are within of the uncertainty of the measurements. Furthermore, it is also observed that when the temperature is increased, the values of contact angle drops. Thus, at working temperature of the EV transmissions (around 393 K), the contact angle will be lower implying a superior wettability and the creation of a tribo-film that may prevent direct surface contact [51]. However, the effects of nanoadditives on wetting have not yet been explained and need to be better understood.

Marques et al. [17] previously studied the surface tension and contact angle of four PAO base oils (PAO6, PAO20, PAO32 and PAO40) at 293.15 to 323.15 K, finding the same trends for viscosities, surface tensions and contact angles of PAOs. Kalin et al. [52,53] also investigated the wetting properties between some engineering surfaces (steel and several types of DLC coatings) and PAO9. These authors obtained a steady-state contact angle of 11.3° for PAO9 on the surface of steel AISI 52100 at room temperature. In the current work, a lower contact angle value has been obtained for PAO8 at room temperature (298 K), around 8°. So, the higher the molecular mass (or the viscosity grade) of the PAOs, the greater the contact angle. This result is in line with that reported by Marques et al. [17].

Concerning the rheological tests, the flow curves for the PAO8 base lubricant as well as for both types of nanolubricants (Fig. 10) at the studied mass fractions (0.05, 0.10, 0.15 and 0.20 wt%) and temperatures show linear dependence of the shear stress (τ) and shear rate (γ), the shear viscosity being the slope of such relationship. Thus, the base oil and the nanolubricants exhibit Newtonian behavior. Consequently, there is no influence of the shear rate on the viscosity for each lubricant, i.e., it is possible to determine a single viscosity value at each studied temperature without considering the flow conditions. As can be seen in Fig. 10, there is a slight increment of the viscosity with the mass fraction,

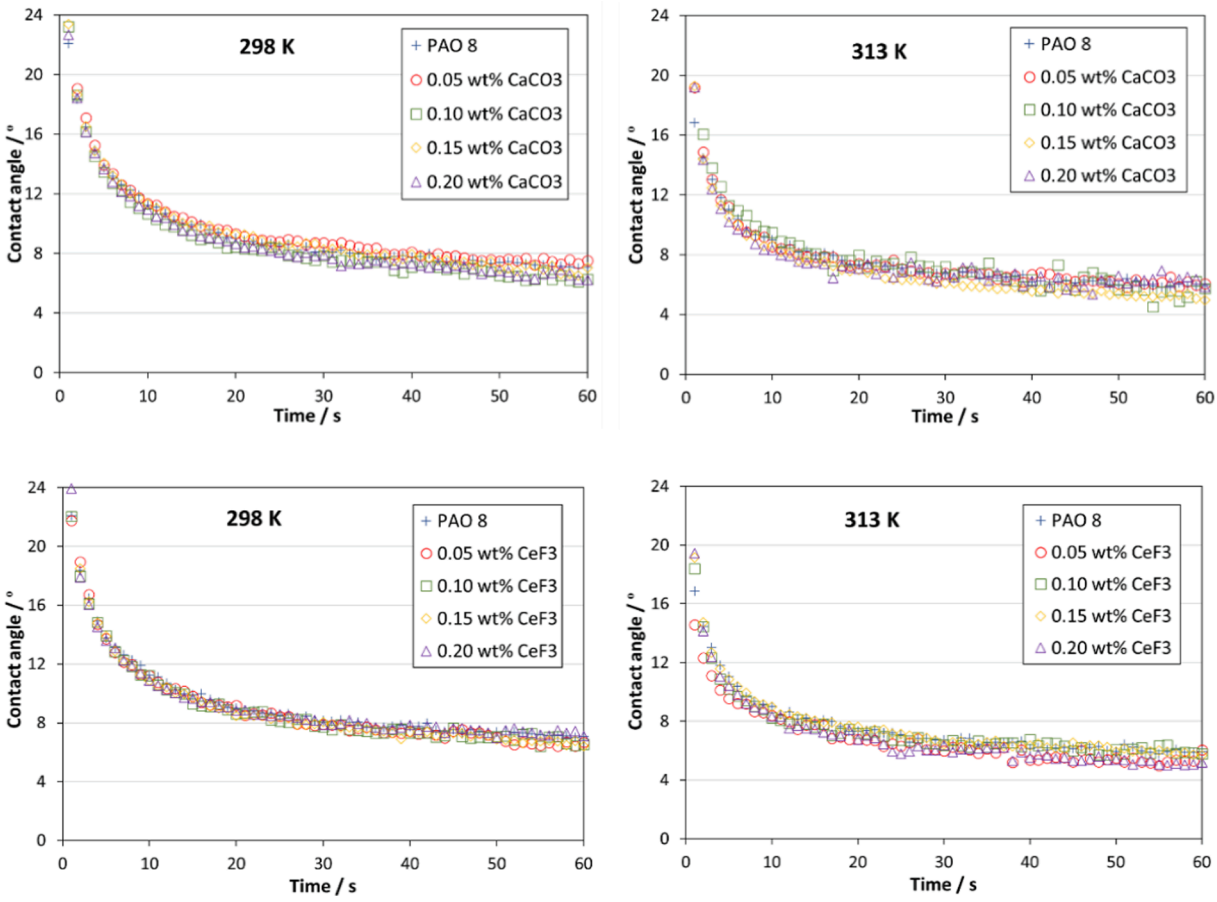

Fig. 9. Contact angle measurements obtained for the base oil and $CaCO_3$ and CeF_3 nanolubricants at 298 and 313 K.

which can be considered negligible considering the studied range of the nanoparticle concentrations. As expected, temperature has a strong effect on viscosity, decreasing by up to one order of magnitude between 293.15 and 363.15 K.

3.3. Friction and wear results

Friction tests were carried out in the tribometer for the nanolubricants of PAO8 with 0.05 wt%, 0.10 wt%, 0.15 wt% or 0.20 wt% in $CaCO_3$ or CeF_3 NPs. Mean values of the coefficient of friction, μ, were obtained (Fig. 11 and Table 3) for each of the studied lubricants. The μ value for the PAO8 base oil has been previously measured [38], for the same operating conditions. As it can be observed in Fig. 11 and in Table 3, the addition of NPs as base oil additives leads to a reduction in the friction coefficient with respect to the oil without additives, reaching decreases of 13 % for the optimal concentration of $CaCO_3$ NPs (0.05 wt %) and 10 % for that of CeF_3 NPs (0.10 wt%). It is evidently seen that for both types of nanolubricants the NP concentration influences the antifriction behavior. Thus, at concentrations higher than the optimum for both NPs, the stability of nanolubricants is poorer and may cause problems of nanoparticle agglomeration at the contact area, because if the nanoparticle concentration is too high, nanoparticle deposition may create new asperities and thus increase the friction [28].

Concerning the wear produced during friction tests, the profile measurements show notable wear improvements in tested pins lubricated with nanolubricants with respect to those lubricated with PAO8 without additives (Fig. 12 and Table 3). Specifically, for nanolubricants containing $CaCO_3$ NPs, improvements of 28 % in WSD (0.15 wt%), 41 % in WTD (0.10 wt%) and 59 % in the area of the wear track (0.15 wt%) are achieved; while that for lubricants PAO8 + CeF_3 NPs, improvements of 19 % in WSD (0.20 wt%), 53 % in WTD (0.10 wt%) and 58 % for the area of the worn tread (0.20 wt%) are obtained. Fig. 13 shows the 3D profile and its vertical section obtained for the PAO8 base oil [38], its optimal nanolubricants with $CaCO_3$ NPs (0.15 wt%) or with CeF_3 NPs (0.20 wt%). Excellent wear reduction can be observed for both nanolubricants. Thus, it can be concluded that both NPs have good antiwear ability.

Moreover, the roughness (Ra) of worn tracks of pins was examined to get more information about the antiwear properties of $CaCO_3$ and CeF_3 NPs. Worn pins lubricated with both types of nanolubricants are less rough than those lubricated with PAO8 without additives (Table 4).

Specifically, a Ra value of 18.8 nm was observed for the worn track lubricated with PAO8, whereas the smallest Ra values (16.8 and 16.9 nm) were obtained for the surface correlated with the 0.15 wt% $CaCO_3$ and 0.20 wt% CeF_3 nanolubricants, resulting in a roughness reduction of about 10 %. These results suggest that both nanopowders improve the surface contact area compared to the base oil, which may be due to a surface repair mechanism.

Finally, to obtain information on the distribution of NPs in worn tracks to detect the function that NPs play in reducing wear, after

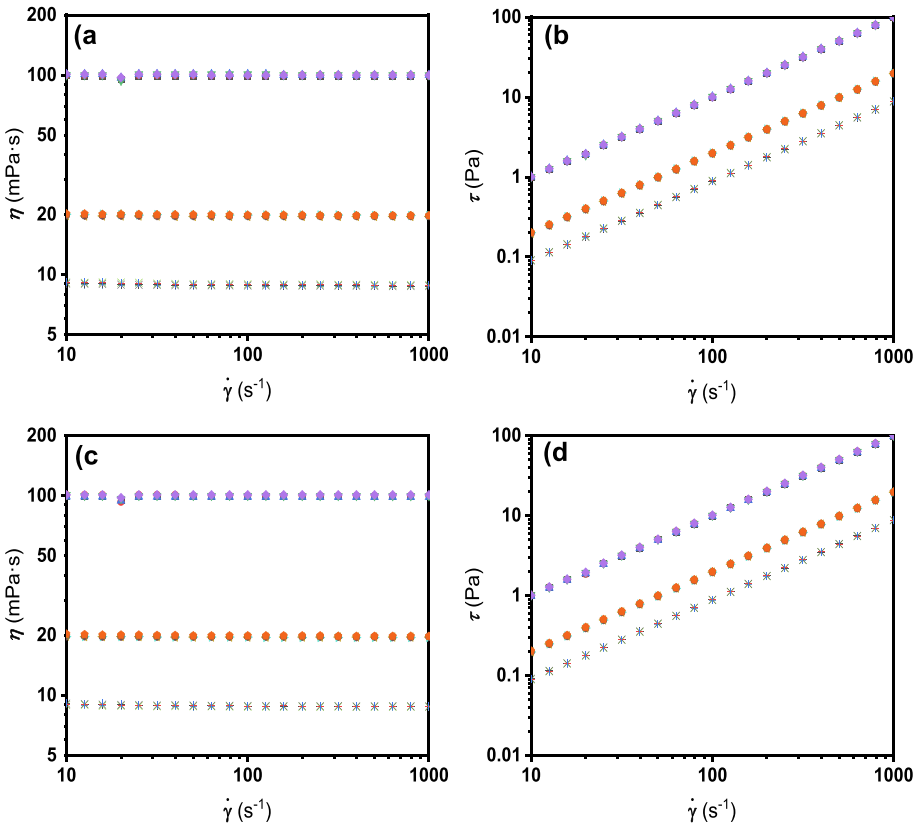

Fig. 10. Flow curves of $CaCO_3$/PAO8 (a-b) and CeF_3/PAO8 (c-d) nanolubricants: viscosity (a,c) and shear stress (b,d) as function of the shear rate at temperatures of 293.15 K (0 wt% ■, 0.05 wt% ●, 0.10 wt% ▲, 0.15 wt% ▼, 0.20 wt% ◆), 333.15 K (0 wt% ◀, 0.05 wt% ▶, 0.10 wt% ⬢, 0.15 wt% ★, 0.20 wt% ⬟), and 363.15 K (0 wt% +, 0.05 wt% ×, 0.10 wt% ✳, 0.15 wt% –, 0.20 wt% |).

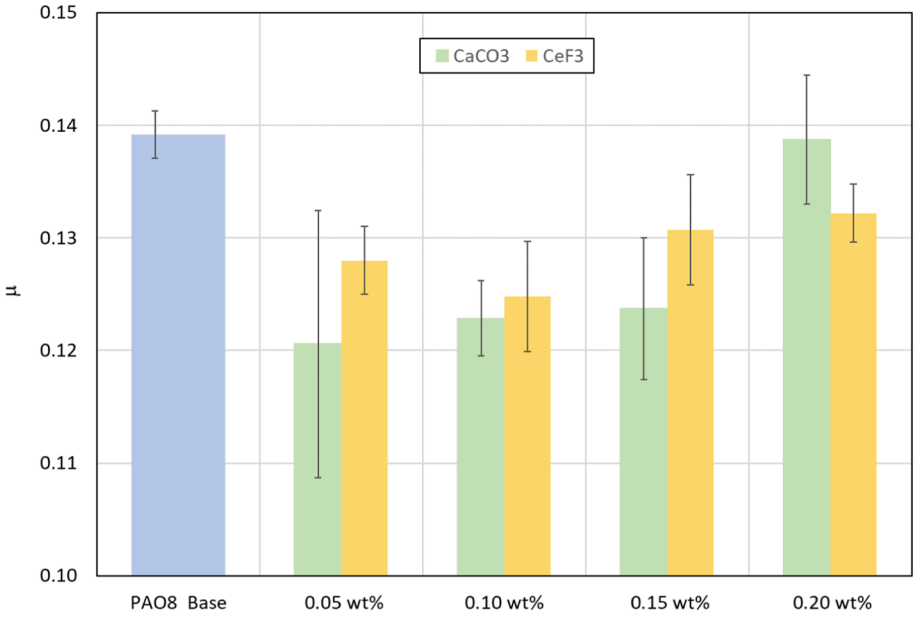

Fig. 11. Comparison between mean friction coefficients (μ) found with PAO8 base oil [38] as well as its nanolubricants containing $CaCO_3$ or CeF_3 NPs at 393.15 K.

Table 3
Average friction coefficient, μ, average wear scar diameter, WSD, average wear track depth, WTD and average worn area with their standard deviations, σ, for the tested PAO8 lubricants at 393.15 K.

Lubricant	μ	σ	WSD/μm	σ/μm	WTD/μm	σ/μm	Area/ μm^2	σ/ μm^2
PAO8 [38]	0.139	0.002	392	14	2.35	0.17	605	52
+ 0.05 wt% $CaCO_3$	0.121	0.012	361	20	1.86	0.22	454	82
+ 0.10 wt% $CaCO_3$	0.123	0.003	331	36	1.38	0.21	294	54
+ 0.15 wt% $CaCO_3$	0.124	0.006	283	31	1.52	0.02	248	57
+ 0.20 wt% $CaCO_3$	0.139	0.006	347	31	1.53	0.33	358	94
+ 0.05 wt% CeF_3	0.128	0.003	381	46	2.05	0.41	589	62
+ 0.10 wt% CeF_3	0.125	0.005	319	21	1.11	0.47	264	51
+ 0.15 wt% CeF_3	0.131	0.005	356	13	1.91	0.18	472	50
+ 0.20 wt% CeF_3	0.132	0.003	316	14	1.15	0.15	252	36

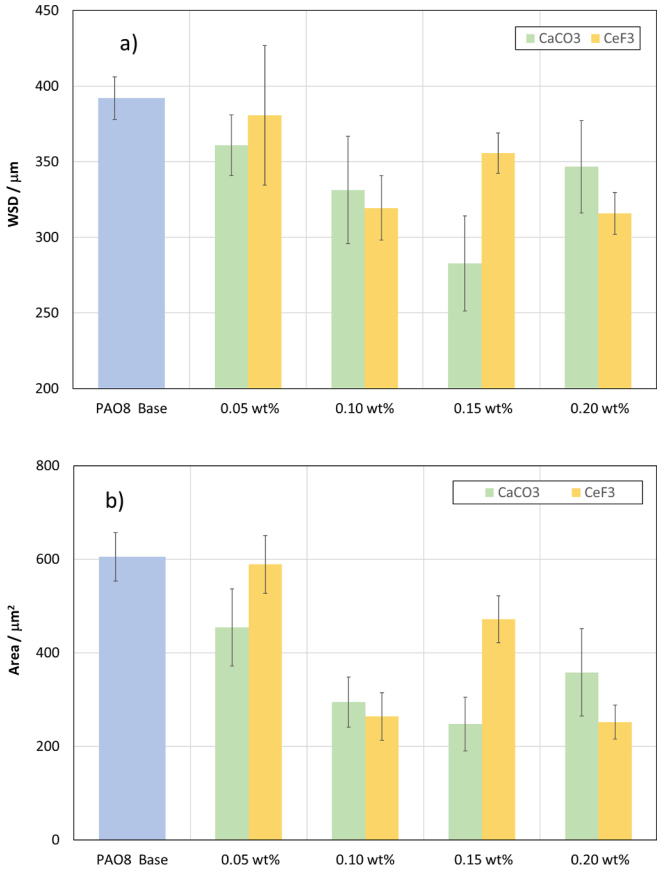

Fig. 12. Mean a) wear scar diameters and b) worn areas of the tested pins achieved with PAO8 base oil and with the formulated nanolubricants.

friction tests, Raman mappings of the worn surfaces were recorded with a confocal Raman microscope (532 nm). Previously, the Raman spectra were obtained for all the components of the nanolubricants: PAO8 base oil [38] as well as CeF_3 and $CaCO_3$ NPs (Fig. 4), to recognize the components in the mapping. Therefore, mappings of the worn tracks lubricated with the nanolubricants with the best anti-wear behavior, PAO8 + 0.20 wt% CeF_3 NPs, and PAO8 + 0.15 wt% $CaCO_3$ NPs were carried out. Fig. 14a shows the relevant areas in red and blue, in which the spectrum coincides with that obtained for CeF_3 NPs or PAO8, respectively. This information suggests that tribofilm formation (mainly due to PAO8) and repairing (for CeF_3 NPs) mechanisms occurred on the worn surface in friction tests. Regarding the Raman mapping of the track lubricated with the nanolubricant with $CaCO_3$ NPs (Fig. 14b), the spectrum obtained in the red areas coincide with that of the $CaCO_3$ NPs and that obtained in the blue zones with that of PAO8. As in the case of CeF_3 NPs, the mechanism of lubricant tribofilm formation (due to PAO8) and repairing (due to $CaCO_3$ NPs) can also be observed. Therefore, considering these Raman mappings and the previous roughness results two possible mechanisms of wear for both cases can be found: tribofilm formation due to oil, large areas are observed in the direction of sliding, and nanoparticle repairing mechanism, where NPs can be embedded in defects or deformations of the metal surface, thus having a surface repair function. Due to the repairing mechanism, nanoparticles can fill the grooves and scars of the rubbing surface developing in improved surface finish [54,55].

It should be noted that in both Fig. 14a and b, severe abrasion wear is observed in the worn tracks. Usually, abrasive wear occurs when a solid object is loaded against particles of a material that have equal or bigger hardness. In this case, the tribological contact is formed by a two-body, where hard asperities or rigidly held grits pass over the surface like a cutting tool [56].

4. Conclusions

In this research the following results were found:

- Nanolubricants based on PAO8 base oil showed stabilities higher than 48 h.
- Small decreases for nanolubricants in surface tension were obtained with reductions of 0.16 % ($T = 298.15$ K) and 0.26 % ($T = 313.15$ K) for 0.15 wt% of CeF_3 and 0.64 % ($T = 298.15$ K) and 0.67 % ($T = 313.15$ K) for 0.10 wt% of $CaCO_3$.
- In rheological tests, all nanolubricants and base oil exhibit Newtonian behavior.
- Friction coefficients for all the nanolubricants are shorter than for the PAO8 base oil: maximum reductions of 13 % for $CaCO_3$ NPs (0.05 wt %) and 10 % for CeF_3 NPs (0.10 wt%).
- For all the nanolubricants the wear in pins is lower for the PAO8: maximum improvements of 28 % in WSD (0.15 wt% $CaCO_3$ NPs) and 19 % in WSD (0.20 wt% CeF_3 NPs) are found.
- Through Raman, the repairing surface, tribofilm formation and rolling mechanisms owing to the nanopowders were suggested.

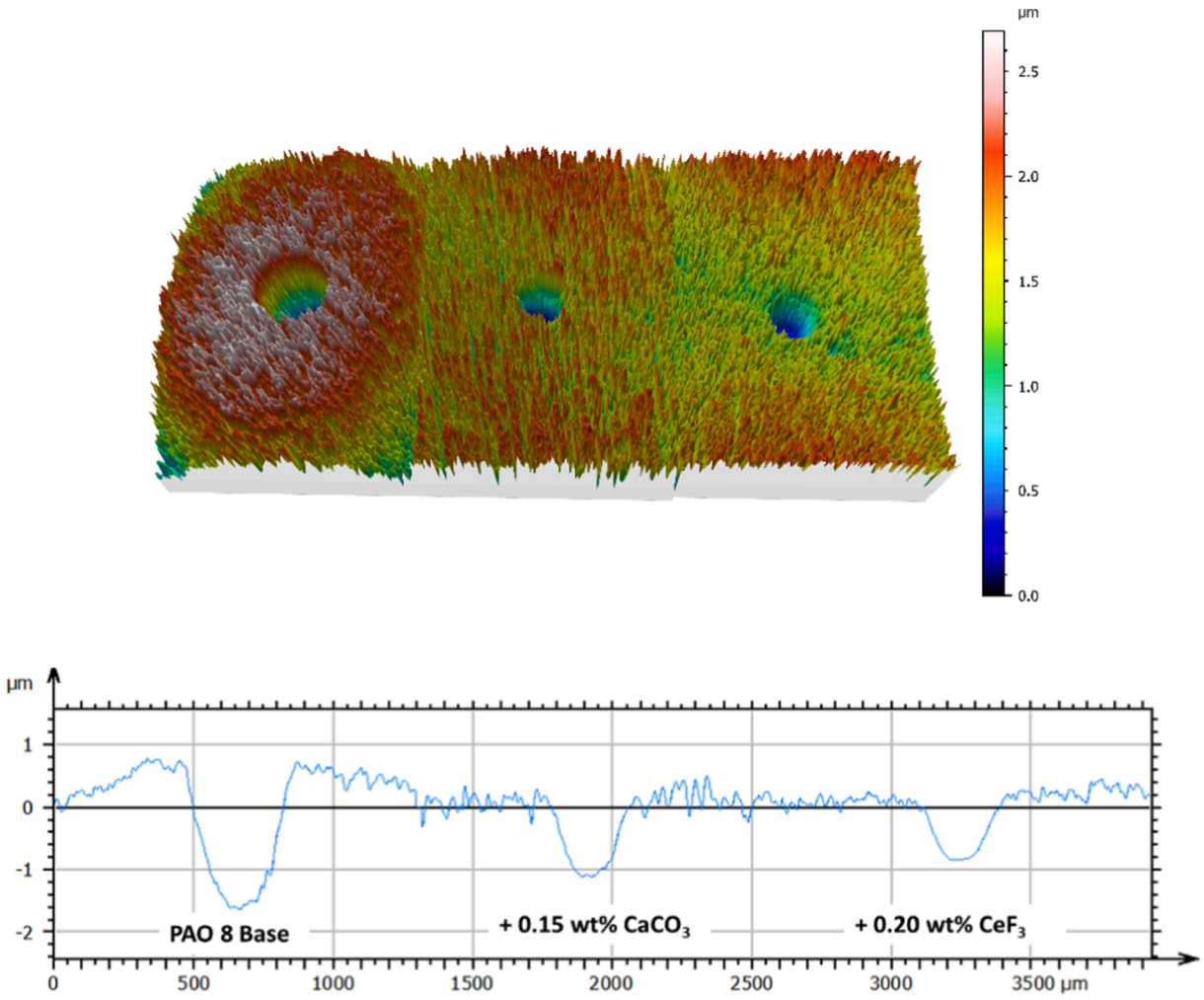

Fig. 13. 3D Surface topography of worn surfaces and cross section profiles of worn surfaces lubricated with PAO8 base oil and the optimum $CaCO_3$ and CeF_3 nanolubricants.

Table 4
Mean roughness parameter Ra and its uncertainties, σ, in worn pins tested by PAO8 lubricants (Gaussian filter: 0.08 mm cut-off).

Lubricant	Ra/nm	σ/nm
PAO8 [38]	18.8	1.7
+ 0.05 wt% $CaCO_3$	18.7	1.8
+ 0.10 wt% $CaCO_3$	17.4	1.3
+ 0.15 wt% $CaCO_3$	16.8	1.4
+ 0.20 wt% $CaCO_3$	18.3	1.2
+ 0.05 wt% CeF_3	18.7	1.3
+ 0.10 wt% CeF_3	17.9	1.6
+ 0.15 wt% CeF_3	17.8	1.4
+ 0.20 wt% CeF_3	16.9	1.3

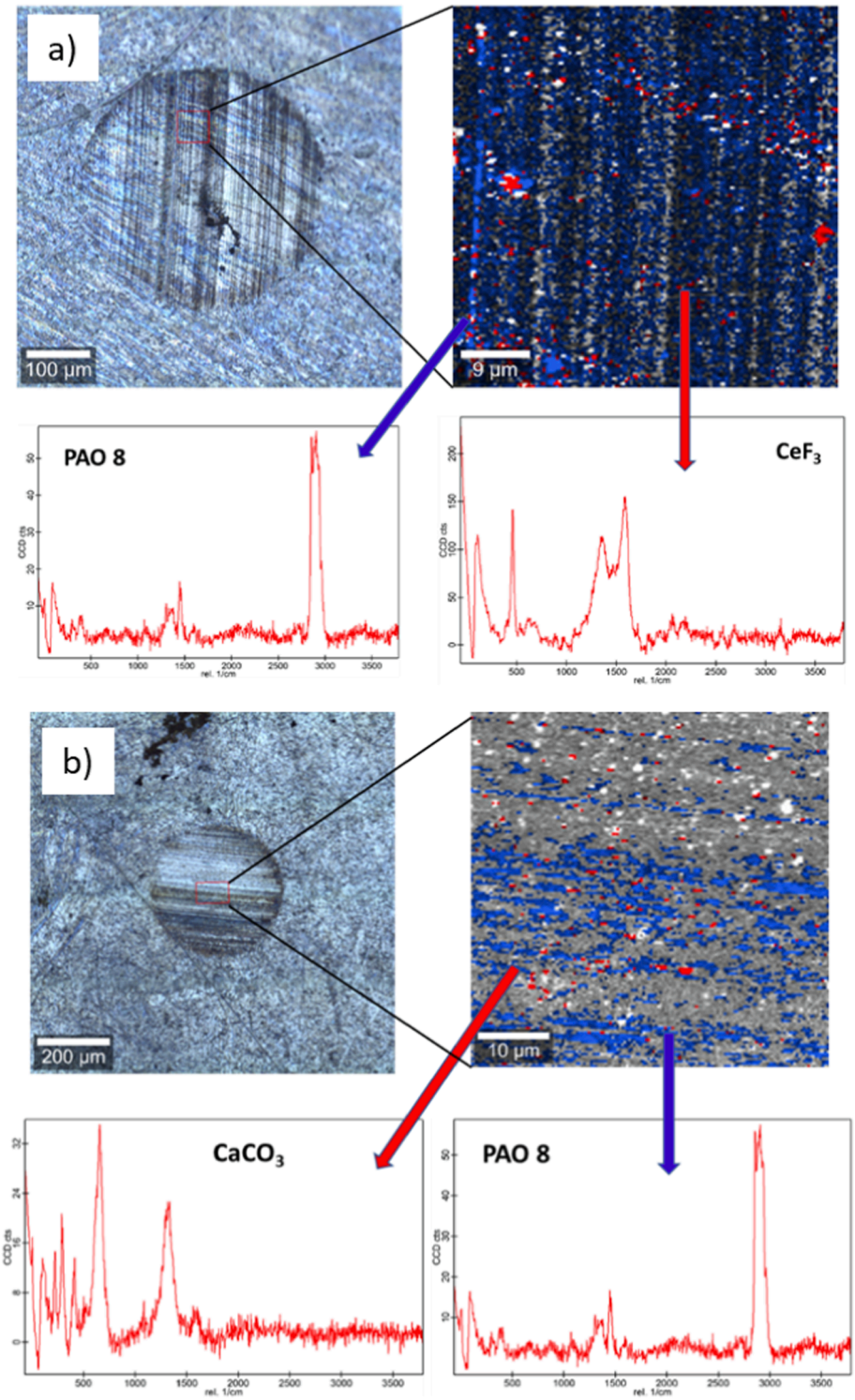

Fig. 14. Mapping Raman of worn surface tested with a) 0.20 wt% CeF_3 nanolubricant and b) 0.20 wt% $CaCO_3$ nanolubricant.

CRediT authorship contribution statement

José M. Liñeira del Río: Conceptualization, Investigation, Methodology, Writing – original draft, Writing – review & editing. **A. Alba:** Conceptualization, Investigation, Methodology. **M.J.G. Guimarey:** Conceptualization, Investigation, Methodology. **Jose I. Prado:** Conceptualization, Investigation, Methodology. **Alfredo Amigo:** Formal analysis, Supervision, Validation, Writing – review & editing. **Josefa Fernández:** Supervision, Validation, Project administration, Funding acquisition, Writing – review & editing.

Declaration of Competing Interest

The authors declare that they have no known competing financial interests or personal relationships that could have appeared to influence the work reported in this paper.

Data availability

Data will be made available on request.

Acknowledgments

This research is supported by Xunta de Galicia (ED431C 2020/10), by MCIN/AEI/10.13039/501100011033 through the PID2020-112846RB-C22 project. JMLdR is grateful for financial support through the Margarita Salas program, funded by MCIN/AEI/10.13039/501100011033 and "NextGenerationEU/PRTR". Dr. M.J.G.G. acknowledges a postdoctoral fellowship (ED481B-2019-015) from the Xunta de Galicia (Spain). Furthermore, authors are also grateful to REPSOL Lubricants for providing the PAO8 base oil and to RIAIDT-USC for its analytical facilities.

References

[1] L.I. Farfan-Cabrera, Tribology of electric vehicles: A review of critical components, current state and future improvement trends, Tribol. Int. 138 (2019) 473–486, https://doi.org/10.1016/j.triboint.2019.06.029.
[2] L.I. Farfan-Cabrera, A. Erdemir, J.A. Cao-Romero-Gallegos, I. Alam, S. Lee, Electrification effects on dry and lubricated sliding wear of bearing steel interfaces, Wear 516 (2023), 204592, https://doi.org/10.1016/j.wear.2022.204592.
[3] A. García Tuero, N. Rivera, E. Rodríguez, A. Fernández-González, J.L. Viesca, A. Hernández Battez, Influence of additives concentration on the electrical properties and the tribological behaviour of three automatic transmission fluids, Lubricants 10 (2022) 276, https://doi.org/10.3390/lubricants10110276.
[4] E. Rodríguez, N. Rivera, A. Fernández-González, T. Pérez, R. González, A.H. Battez, Electrical compatibility of transmission fluids in electric vehicles, Tribol. Int. 171 (2022), 107544, https://doi.org/10.1016/j.triboint.2022.107544.
[5] W. Ahmed Abdalglil Mustafa, F. Dassenoy, M. Sarno, A. Senatore, A review on potentials and challenges of nanolubricants as promising lubricants for electric vehicles, Lubr. Sci. 34 (2022) 1–29, https://doi.org/10.1002/ls.1568.
[6] K. Narita, D. Takekawa, Lubricants technology applied to transmissions in hybrid electric vehicles and electric vehicles, SAE Technical Paper (2019), https://doi.org/10.4271/2019-01-2338.
[7] M. Gulzar, H.H. Masjuki, M.A. Kalam, M. Varman, N.W.M. Zulkifli, R.A. Mufti, R. Zahid, Tribological performance of nanoparticles as lubricating oil additives, J. Nanopart. Res. 18 (2016) 223, https://doi.org/10.1007/s11051-016-3537-4.
[8] S. Shahnazar, S. Bagheri, S.B. Abd Hamid, Enhancing lubricant properties by nanoparticle additives, Int. J. Hydrogen Energy 41 (2016) 3153–3170, https://doi.org/10.1016/j.ijhydene.2015.12.040.
[9] A. Singh, N. Verma, T.G. Mamatha, A. Kumar, S. Singh, K. Kumar, Properties, functions and applications of commonly used lubricant additives: A review, Mater. Today:. Proc. 44 (2021) 5018–5022, https://doi.org/10.1016/j.matpr.2021.01.029.
[10] S.B. Mousavi, S.Z. Heris, P. Estellé, Experimental comparison between ZnO and MoS2 nanoparticles as additives on performance of diesel oil-based nano lubricant, Sci. Rep. 10 (2020) 5813, https://doi.org/10.1038/s41598-020-62830-1.
[11] S.B. Mousavi, S. Zeinali Heris, P. Estellé, Viscosity, tribological and physicochemical features of ZnO and MoS2 diesel oil-based nanofluids: An experimental study, Fuel 293 (2021), 120481, https://doi.org/10.1016/j.fuel.2021.120481.
[12] S.B. Mousavi, S. Zeinali Heris, Experimental investigation of ZnO nanoparticles effects on thermophysical and tribological properties of diesel oil, Int. J. Hydrogen Energy 45 (2020) 23603–23614, https://doi.org/10.1016/j.ijhydene.2020.05.259.
[13] N.G. Demas, E.V. Timofeeva, J.L. Routbort, G.R. Fenske, Tribological effects of BN and MoS_2 nanoparticles added to polyalphaolefin oil in piston skirt/cylinder liner tests, Tribol. Lett. 47 (2012) 91–102, https://doi.org/10.1007/s11249-012-9965-0.
[14] Z. Tang, S. Li, A review of recent developments of friction modifiers for liquid lubricants (2007–present), Curr. Opin. Solid State Mater. Sci. 18 (2014) 119–139, https://doi.org/10.1016/j.cossms.2014.02.002.
[15] H. Spikes, Friction modifier additives, Tribol. Lett. 60 (2015) 5, https://doi.org/10.1007/s11249-015-0589-z.
[16] D. Blanco, M. Bartolomé, B. Ramajo, J.L. Viesca, R. González, A. Hernández Battez, Wetting properties of seven phosphonium cation-based ionic liquids, Ind. Eng. Chem. Res. 55 (2016) 9594–9602, https://doi.org/10.1021/acs.iecr.6b00821.
[17] M.A. Coelho de Sousa Marques, M.J.G. Guimarey, V. Domínguez-Arca, A. Amigo, J. Fernández, Heat capacity, density, surface tension, and contact angle for polyalphaolefins and ester lubricants, Thermochim. Acta 703 (2021), 178994, https://doi.org/10.1016/j.tca.2021.178994.
[18] P. Estellé, D. Cabaleiro, G. Żyła, L. Lugo, S.M.S. Murshed, Current trends in surface tension and wetting behavior of nanofluids, Renew. Sustain. Energy Rev. 94 (2018) 931–944, https://doi.org/10.1016/j.rser.2018.07.006.
[19] S.J. Kim, I.C. Bang, J. Buongiorno, L. Hu, Effects of nanoparticle deposition on surface wettability influencing boiling heat transfer in nanofluids, Appl. Phys. Lett. 89 (2016), 153107, https://doi.org/10.1063/1.2360892.
[20] S. Vafaei, T. Borca-Tasciuc, M.Z. Podowski, A. Purkayastha, G. Ramanath, P. M. Ajayan, Effect of nanoparticles on sessile droplet contact angle, Nanotechnology 17 (2006) 2523–2527, https://doi.org/10.1088/0957-4484/17/10/014.
[21] A.D. Thampi, M.A. Prasanth, A.P. Anandu, E. Sneha, B. Sasidharan, S. Rani, The effect of nanoparticle additives on the tribological properties of various lubricating oils – Review, Mater. Today:. Proc. 47 (2021) 4919–4924, https://doi.org/10.1016/j.matpr.2021.03.664.
[22] F. Mariño, J.M. Liñeira del Río, E.R. López, J. Fernández, Chemically modified nanomaterials as lubricant additive: Time stability, friction, and wear, J. Mol. Liq. 382 (2023), 121913, https://doi.org/10.1016/j.molliq.2023.121913.
[23] C. Kumara, D.N. Leonard, H.M. Meyer, H. Luo, B.L. Armstrong, J. Qu, Palladium Nanoparticle-Enabled Ultrathick Tribofilm with Unique Composition, ACS Appl. Mater. Interfaces 10 (2018) 31804–31812, https://doi.org/10.1021/acsami.8b11213.
[24] R.A.E. Wright, K. Wang, J. Qu, B. Zhao, Oil-soluble polymer brush grafted nanoparticles as effective lubricant additives for friction and wear reduction, Angew. Chem. Int. Ed. 55 (2016) 8656–8660, https://doi.org/10.1002/anie.201603663.
[25] B.T. Seymour, R.A.E. Wright, A.C. Parrott, H. Gao, A. Martini, J. Qu, S. Dai, B. Zhao, Poly(alkyl methacrylate) brush-grafted silica nanoparticles as oil lubricant additives: effects of alkyl pendant groups on oil dispersibility, stability, and lubrication property, ACS Appl. Mater. Interfaces 9 (2017) 25038–25048, https://doi.org/10.1021/acsami.7b06714.
[26] M. Kalin, J. Kogovšek, M. Remškar, Mechanisms and improvements in the friction and wear behavior using MoS2 nanotubes as potential oil additives, Wear 280–281 (2012) 36–45, https://doi.org/10.1016/j.wear.2012.01.011.
[27] C.C.Y. Kwak, A. Adhvaryu, X. Fang, et al., Understanding base oils and lubricants for electric drivetrain applications, SAE Technical Paper 2019–01-2337 (2019), https://doi.org/10.4271/2019-01-2337.
[28] M.N. Çöl, O.N. Celik, A. Sert, Tribological behaviours of lubricating oils with CNT and Si_3N_4 nanoparticle additives, Arch. Mater. Sci. Eng. 67 (2014) 53–59.
[29] S. Razavi, S. Sabbaghi, K. Rasouli, Comparative investigation of the influence of CaCO3 and SiO2 nanoparticles on lithium-based grease: Physical, tribological, and rheological properties, Inorg. Chem. Commun. 142 (2022), 109601, https://doi.org/10.1016/j.inoche.2022.109601.
[30] C. Wu, Y. Xie, H. Zhao, H. Yang, X. Li, J. Ni, Effects of hBN and $CaCO_3$ nanoparticles on tribological and vibration properties of polyurea grease on rolling bearing, Tribol. Lett. 70 (2022) 95, https://doi.org/10.1007/s11249-022-01639-7.
[31] K. Akhtar, S. Yousafzai, Tribological and rheological properties of the ultrafine CaCO3 blended nano grease, J. Dispers. Sci. Technol. 43 (2022) 408–418, https://doi.org/10.1080/01932691.2020.1842757.
[32] K. Vyavhare, R.B. Timmons, A. Erdemir, P.B. Aswath, Tribological interaction of plasma-functionalized CaCO3 nanoparticles with zinc and ashless dithiophosphate additives, Tribol. Lett. 69 (2021) 49, https://doi.org/10.1007/s11249-021-01423-z.
[33] C. Gu, Q. Li, Z. Gu, G. Zhu, Study on application of CeO2 and CaCO3 nanoparticles in lubricating oils, J. Rare Earths 26 (2008) 163–167, https://doi.org/10.1016/S1002-0721(08)60058-7.
[34] Q. Sunqing, D. Junxiu, C. Guoxu, Wear and Friction Behaviour of CaCO3 Nanoparticles Used as Additives in Lubricating Oils, Lubr. Sci. 12 (2000) 205–212, https://doi.org/10.1002/ls.3010120207.
[35] M. Zhang, X. Wang, X. Fu, Y. Xia, Performance and anti-wear mechanism of CaCO3 nanoparticles as a green additive in poly-alpha-olefin, Tribol. Int. 42 (2009) 1029–1039, https://doi.org/10.1016/j.triboint.2009.02.012.
[36] T. Kulkarni, B. Toksha, A. Chatterjee, J. Naik, A. Autee, Anti-wear (AW) and extreme-pressure (EP) behavior of jojoba oil dispersed with green additive CaCO3 nanoparticles, J. Eng. Appl. Sci. 70 (2023) 29, https://doi.org/10.1186/s44147-023-00202-y.
[37] Q. Sunqing, D. Junxiu, C. Guoxu, Tribological properties of CeF3 nanoparticles as additives in lubricating oils, Wear 230 (1999) 35–38, https://doi.org/10.1016/S0043-1648(99)00084-8.
[38] J.M. Liñeira del Río, F. Mariño, E.R. López, D.E.P. Gonçalves, J.H.O. Seabra, J. Fernández, Tribological enhancement of potential electric vehicle lubricants using coated TiO2 nanoparticles as additives, J. Mol. Liq. 371 (2023), 121097, https://doi.org/10.1016/j.molliq.2022.121097.
[39] A.I. Hussein, Z. Ab-Ghani, A.N. Che Mat, N.A. Ab Ghani, A. Husein, I.J.A.S. Ab Rahman, Synthesis and characterization of spherical calcium carbonate nanoparticles derived from cockle shells, Appl. Sci. 10 (2020) 7170, https://doi.org/10.3390/app10207170.
[40] Y. Wang, Y.X. Moo, C. Chen, P. Gunawan, R. Xu, Fast precipitation of uniform CaCO3 nanospheres and their transformation to hollow hydroxyapatite nanospheres, J. Colloid Interface Sci. 352 (2010) 393–400, https://doi.org/10.1016/j.jcis.2010.08.060.
[41] Z. Yuan, D. Zhang, G. Fan, Y. Chen, Y. Fan, B. Liu, Synergistic effect of CeF3 nanoparticles supported on Ti3C2 MXene for catalyzing hydrogen storage of NaAlH4, ACS Appl. Energy Mater. 4 (2021) 2820–2827, https://doi.org/10.1021/acsaem.1c00122.
[42] Deepika, S.K. Hait, Y.J.J.O.C.T. Chen, Research, Optimization of milling parameters on the synthesis of stearic acid coated CaCO3 nanoparticles, J. Coat. Technol. Res. 11 (2014) 273–282, https://doi.org/10.1007/s11998-013-9547-6.
[43] S.B. Mousavi, S. Zeinali Heris, M.G. Hosseini, Experimental investigation of MoS2/diesel oil nanofluid thermophysical and rheological properties, Int. Commun. Heat Mass Transfer 108 (2019), 104298, https://doi.org/10.1016/j.icheatmasstransfer.2019.104298.

[44] M.İ. Kati, Behaviour of radio-thermoluminescence (X-ray irradiated), thermal and structural characterization of limestone, Celal Bayar Univ. J. Sci. 18 (2022) 435–441, https://doi.org/10.18466/cbayarfbe.1106810.
[45] Zeitschrift für physikalische Chemie. Abteilung B, Zeitschrift für physikalische Chemie. Abteilung B, 1928.
[46] A. Weissberger, & B.W. Rossiter, Physical Methods of Chemistry: Electrochemical Methods, 1971.
[47] D. Cabaleiro, M.J. Pastoriza-Gallego, C. Gracia-Fernández, M.M. Piñeiro, L. Lugo, Rheological and volumetric properties of TiO2-ethylene glycol nanofluids, Nanoscale Res. Lett. 8 (2013) 286, https://doi.org/10.1186/1556-276X-8-286.
[48] P. Heyer, J. Läuger, Correlation between friction and flow of lubricating greases in a new tribometer Device, Lubr. Sci. 21 (2009) 253–268, https://doi.org/10.1002/ls.88.
[49] K.I. Nasser, J.M. Liñeira del Río, E.R. López, J. Fernández, Synergistic effects of hexagonal boron nitride nanoparticles and phosphonium ionic liquids as hybrid lubricant additives, J. Mol. Liq. 311 (2020), 113343, https://doi.org/10.1016/j.molliq.2020.113343.
[50] J.M. Liñeira del Río, E.R. López, M. González Gómez, S. Yáñez Vilar, Y. Piñeiro, J. Rivas, D.E.P. Gonçalves, J.H.O. Seabra, J. Fernández, Tribological behavior of nanolubricants based on coated magnetic nanoparticles and trimethylolpropane trioleate base oil, Nanomaterials 10 (2020) 683, https://doi.org/10.3390/nano10040683.
[51] M.F. Bin Abdollah, H. Amiruddin, M. Alif Azmi, N.A. Mat Tahir, Lubrication mechanisms of hexagonal boron nitride nano-additives water-based lubricant for steel–steel contact, Proc. Institut. Mech. Eng. Part J: J. Eng. Tribol. 235 (2020) 1038–1046, https://doi.org/10.1177/1350650120940173.
[52] M. Kalin, M. Polajnar, The effect of wetting and surface energy on the friction and slip in oil-lubricated contacts, Tribol. Lett. 52 (2013) 185–194, https://doi.org/10.1007/s11249-013-0194-y.
[53] M. Kalin, M. Polajnar, The wetting of steel, DLC coatings, ceramics and polymers with oils and water: The importance and correlations of surface energy, surface tension, contact angle and spreading, Appl. Surf. Sci. 293 (2014) 97–108, https://doi.org/10.1016/j.apsusc.2013.12.109.
[54] U. Maurya, V. Vasu, D. Kashinath, Three-way compatibility study among nanoparticles, ionic liquid, and dispersant for potential in lubricant formulation, Mater. Today: Proc. 59 (2022) 1651–1658, https://doi.org/10.1016/j.matpr.2022.03.329.
[55] V. Saini, J. Bijwe, S. Seth, S.S.V. Ramakumar, Interfacial interaction of PTFE submicron particles in oil with steel surfaces as excellent extreme-pressure additive, J. Mol. Liq. 325 (2021), 115238, https://doi.org/10.1016/j.molliq.2020.115238.
[56] K.P. Lijesh, M.M. Khonsari, Characterization of abrasive wear using degradation coefficient, Wear 450–451 (2020), 203220, https://doi.org/10.1016/j.wear.2020.203220.
[57] Commission Decision (EU) 2018/1702 of 8 November 2018 establishing the EU Ecolabel criteria for lubricants (notified under document C(2018) 7125), https://eur-lex.europa.eu/eli/dec/2018/1702/oj (Accessed 27 September 2023).